Re-evaluation of magma compositions and processes in the uppermost Critical Zone of the Bushveld Complex

R. GRANT CAWTHORN

Department of Geology, University of the Witwatersrand, Wits, 2050, Republic of South Africa

Abstract

A detailed geochemical study is presented of the uppermost Critical Zone, especially of the footwall and hanging wall to the Merensky Reef, at Impala Platinum Mines in the Bushveld Complex. The approximately 100 m-thick sequence below the Merensky Reef consists of 13 distinct layers which have sharp boundaries. They are adcumulates with varying proportions of cumulus plagioclase, orthopyroxene and chromite.

Experimental studies on the composition of coexisting orthopyroxene liquid indicate that the magma which produced this sequence contained between 4 and 6% MgO. The magma from which the Merensky Reef formed was more evolved than the footwall magma.

Significant variations exist for both the En content of orthopyroxene and mg# number of whole-rock analyses in short vertical sections. Pyroxenite and norite always have higher values than anorthosite. Extremely sharp breaks in these values correlate with changes in modal proportions, and argue against both significant fractionation within the studied interval, and infiltration metasomatism. Quantitative modelling shows that the entire footwall section could have contained pyroxene with a uniform primary composition of En_{82}, and that all the variation now observed reflects the effect of reaction with trapped magma.

Two independent methods for determining the proportion of trapped liquid are presented, based on mg# number and incompatible element abundances. Both yield a uniform proportion in all samples of approximately 10%. Immiscible sulphide liquid from the Merensky Reef can be shown to have infiltrated downwards for <5 m, despite its high density contrast with silicate magma, very low viscosity and low crystallization temperature. Residual silicate magma would have had even more restricted mobility. The migration of residual liquid or fluid through pothole structures in the floor of the Merensky Reef is not supported by the present data.

KEYWORDS: Bushveld Complex, cyclic units, fractionation, trapped liquid.

Introduction

THE fate of interstitial liquid in slowly cooled layered intrusions has been examined by many authors. In the concept summarized by Wager *et al.* (1960) this liquid was assumed to have been trapped to produce a variety of interstitial phases and zoned overgrowths on cumulus minerals. Barnes (1986*a*) presented a quantitative geochemical model of this principle for mafic phases, which rapidly re-equilibrate with interstitial liquid. This was referred to as the trapped liquid shift effect. However, it has also been demonstrated that deformation and compaction could cause migration of interstitial liquid (McKenzie, 1984). Even small proportions of liquid could be squeezed out, provided the time scale is long enough, although this may not be the case in crustal reservoirs. The subsequent reaction of this migrating liquid, with minerals with which it was not originally in equilibrium, was termed infiltration metasomatism by Irvine (1980). A comparison of the relative densities of liquids produced as a result of the crystallization of various assemblages led to the proposal that dense liquid could sink within the crystal pile (Tait *et al.*, 1984). Such processes were seen as being pervasive, but it is also possible that they could become channelized. The latter would decrease the ratio of primary assemblage to

Mineralogical Magazine, February 1996, Vol. 60, pp. 131–148

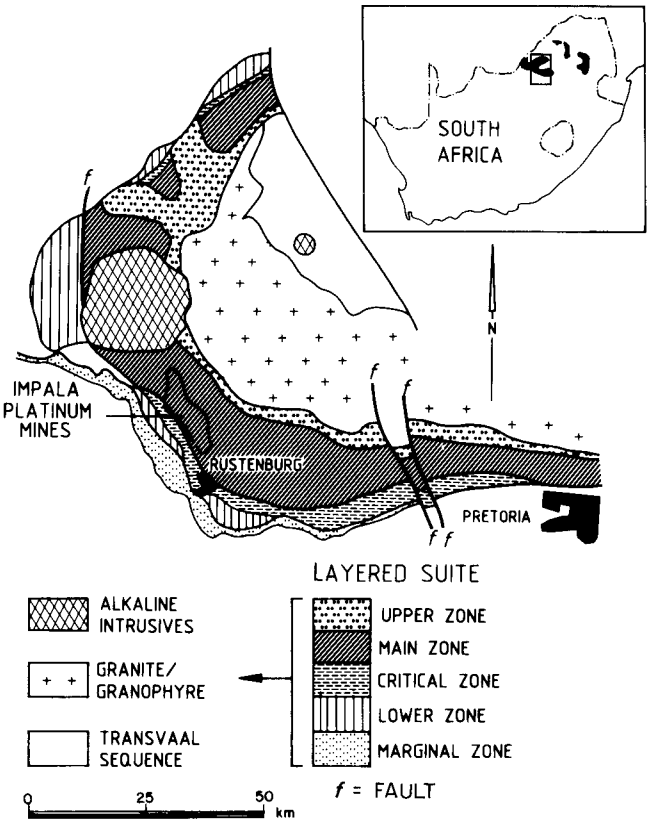

FIG. 1. Simplified geological map of the western Bushveld Complex showing the location of the Impala Platinum Mines.

transgressing liquid, permitting more extensive reaction, ultimately resulting in replacement of some or all of the original mineralogy. Discordant 'finger' structures and larger 'chimneys' have been interpreted as due to upward migration of such interstitial melts (Robins, 1982; Tait and Jaupart, 1992).

All of these processes could, and probably do, occur in different intrusions and under different conditions, and it would be unwise to suggest that only one mechanism applies to all intrusions.

This study focuses on a short vertical section through the uppermost Critical Zone of the Bushveld Complex, and includes geochemical information which throws light on the relative importance of migration *vs.* trapping of residual liquid.

Geological setting

The upper Critical Zone of the Bushveld Complex has been the subject of numerous studies, because of the presence of the Pt-rich Merensky Reef and chromitite layers, and also because it contains some spectacular modal layering with rocks containing different proportions of pyroxene, plagioclase and chromite. Many of these studies have made use of borehole core and mines in the western Bushveld Complex (Fig. 1).

Within the upper Critical Zone a gross cyclicity has been recognised, on a scale from 10 to 100 m, consisting of a basal chromite-rich layer followed by pyroxenite (which may occasionally contain olivine), norite and anorthosite (Eales *et al.*, 1993*a*). Modal plagioclase ranges from <10 to 96%, but the irregular distribution of poikilitic phases in the near-mono-mineralic rocks makes point-counting difficult. The cores of cumulus plagioclase grains range from An_{70-80}, with narrow marginal zoning to An_{50} (Schurmann, 1993). Cumulus orthopyroxene ranges from En_{83-74} (defined as 100*Mg/(Mg+total Fe), becoming more Fe-rich above the Merensky Reef. The compositional variation is discussed in detail

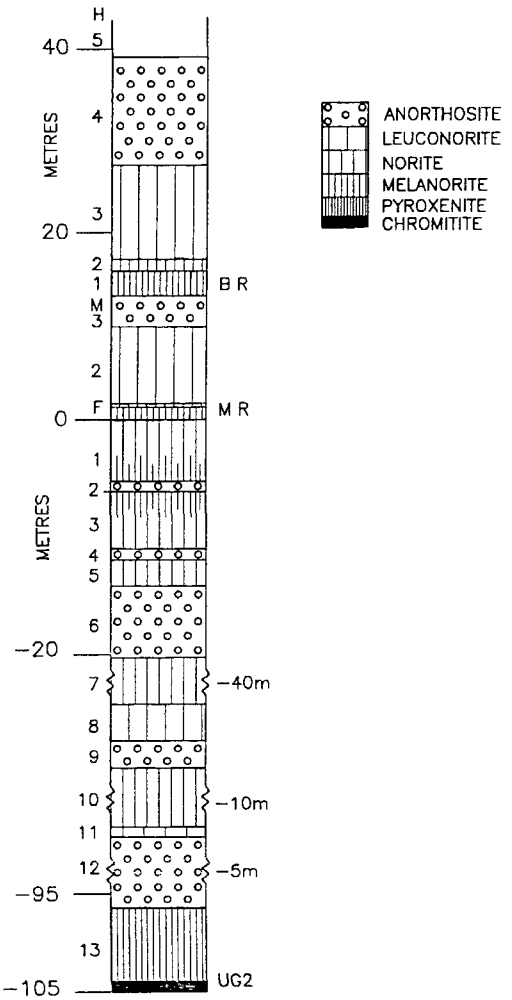

FIG. 2. Schematic section through the uppermost Critical Zone in Impala Platinum Mines. F, M and H refer to footwall, Merensky and hanging wall cyclic units respectively, using the scheme of Leeb-du Toit (1986). UG2, MR and BR refer to Upper Group 2 chromitite layer, Merensky and Bastard Reefs. Note that three intervals (40, 10 and 5 m) of thick homogeneous sequences have been excluded from the footwall succession.

below. At least seven such cyclic units exist. Part of this interval in the Impala Platinum Mines is shown in Fig. 2. Here the Merensky Reef cyclic unit is some 15 m thick, and the underlying cycle, referred to as the Upper Group 2 chromitite cyclic unit (UG2) is >100 m thick (Leeb-du Toit, 1986). It was shown by Eales *et al.* (1986) that rocks in each cycle have a slightly different Sr/Al_2O_3 ratio, and they argued that this was evidence that each cycle was initiated by addition of chemically distinct magma. This conclusion was also reached by Naldrett *et al.* (1986) on the basis of reversals in the En value in orthopyroxene. The interval from the UG2 chromitite to the top of the Critical Zone in the Impala Platinum Mines, has been investigated by Schurmann (1993) who refined the above models on the basis of variations in mineral compositions and proposed emplacement of numerous injections of magma of different compositions into a stratified chamber.

The actual lithological variation within a cyclic unit is, in fact, more complicated than simply chromitite, pyroxenite, norite, followed by anorthosite, as shown in Fig. 2, and a total of 13 continuous layers can be identified in the UG2 cyclic unit (Leeb-du Toit, 1986). At the base is a 6 m-thick pyroxenite, followed by a complex sequence of norite, leuconorite and anorthosite. Contacts are sharp to gradational over a few centimetres between all units. Most units are relatively homogeneous internally, although some modal variation does occur. For example, in the 5 m-thick footwall 3 (F3) there is a gradual upwards increase in pyroxene content (Cawthorn and Poulton, 1988).

In this study, samples were taken from ten bore cores, from the top of the Merensky cyclic unit (M3) down to the top of footwall 7 (F7). Considerable modal variation occurs within this 40 m-thick interval, whereas below this lies a very thick (>40 m) homogeneous norite (F7). Samples have been collected at approximately 1 m intervals. The stratigraphic and petrographic details of this package have been documented elsewhere (Leeb-du Toit, 1986; Schurmann, 1993) and will not be repeated in detail here. It is sufficient to note that the silicate rocks can be classified as adcumulates, consisting of varying proportions of plagioclase and orthopyroxene, with never more than trace contents of chromite, clinopyroxene and biotite. The other feature of importance is the presence of potholes in the base of the Merensky Reef. These are roughly circular features in plan, with variable diameter and depths, but in the Impala Platinum Mines they frequently bottom against the footwall 3 layer (Leeb-du Toit, 1986).

Geochemistry

Samples have been analysed by XRF spectrometry for major and trace elements, and a representative suite from one bore core is presented in Table 1. Analytical precision, based on replicate analysis, is also given in Table 1. As they are almost pure adcumulates containing variable proportions of two minerals, their major element compositions reflect

TABLE 1. Representative whole-rock chemistry of samples from bore core BS1122

Depth*	6.58	5.73	4.31	2.69	1.24	−0.36	−0.61	−1.46	−3.96	−4.86	−5.16	−5.36	−7.06
Unit	M2	M2	M2	M2	M2	F1	F1	F1	F1	F1	F2	F3	F3
SiO_2	50.10	50.24	50.95	50.70	50.43	49.59	49.99	49.22	50.34	51.65	51.57	51.89	51.36
TiO_2	0.08	0.10	0.13	0.10	0.19	0.09	0.09	0.09	0.09	0.14	0.10	0.15	0.12
Al_2O_3	29.68	27.75	25.14	25.26	12.49	25.13	23.55	23.38	23.61	14.47	22.41	15.45	21.46
Fe_2O_3(Tot)	2.14	3.14	4.03	4.09	9.69	4.21	4.61	3.83	4.26	7.56	4.02	7.73	5.18
MnO	0.05	0.05	0.08	0.09	0.17	0.07	0.06	0.09	0.10	0.17	0.10	0.14	0.10
MgO	2.16	3.90	5.66	5.86	17.00	6.26	8.07	7.51	7.86	16.59	9.11	15.83	9.90
CaO	14.65	13.94	13.09	12.73	7.53	12.55	11.80	11.87	12.11	7.92	11.88	8.28	11.00
Na_2O	2.05	2.25	1.81	1.89	1.18	1.80	2.15	1.78	1.72	1.15	1.67	1.20	1.54
K_2O	0.20	0.19	0.18	0.17	0.12	0.18	0.16	0.15	0.15	0.11	0.18	0.15	0.16
P_2O_5	0.02	0.03	0.03	0.03	0.02	0.02	0.03	0.02	0.02	0.02	0.02	0.02	0.03
LOI	0.24	0.13	0.10	0.08	−0.08	0.31	0.38	3.17	0.38	0.15	0.30	0.16	0.45
Total	101.37	101.72	101.20	101.00	100.74	100.21	100.89	101.11	100.64	99.93	101.36	101.00	101.30
Cu	47	44	51	72	293	861	471	18	16	27	16	18	7
Ni	95	116	153	201	26	1616	1040	140	141	381	177	393	225
Rb	3	4	5	4	4	2	4	2	3	4	3	5	3
Sr	359	334	310	318	173	340	329	339	319	206	301	228	276
Zr	20	22	23	19	22	18	21	19	16	21	19	21	20
Y	3	4	4	4	8	3	6	4	6	7	5	5	6
V	31	44	57	51	118	41	49	48	48	82	60	81	60
Cr	159	383	562	552	1936	638	921	913	974	2077	1161	1780	1219
mg#	66.7	71.1	73.6	73.9	77.7	74.6	77.6	79.5	78.5	81.3	81.8	80.2	79.1
IL(Zr)**	13	15	15	13	15	12	14	13	11	14	13	14	13
IL(K)**	13	13	12	11	8	12	11	10	10	7	12	10	11

TABLE 1 *continued*

Depth*	−8.26	−9.16	−9.76	−10.41	−10.90	−11.16	−12.04	−13.34	−14.22	−15.26	−16.35	−17.90	Precision
Unit	F3	F3	F3	F5	F5	F6	F6	F6	F6	F6	F6	F6	
SiO_2	51.32	51.73	50.46	50.93	51.07	48.95	48.44	49.34	49.72	49.26	49.41	49.67	0.34
TiO_2	0.13	0.12	0.09	0.13	0.13	0.05	0.06	0.07	0.06	0.05	0.05	0.06	0.02
Al_2O_3	20.83	22.62	25.65	18.42	21.62	30.90	29.65	27.14	29.55	31.16	32.49	31.52	0.08
Fe_2O_3(Tot)	5.33	4.60	3.36	6.82	5.50	1.31	1.48	3.27	1.49	1.17	0.41	0.75	0.05
MnO	0.10	0.11	0.08	0.15	0.12	0.05	0.03	0.06	0.04	0.02	0.02	0.03	0.01
MgO	10.40	9.33	5.59	12.30	9.81	1.52	2.21	4.99	1.97	1.88	0.95	1.59	0.02
CaO	10.55	11.30	13.32	9.46	11.15	15.27	14.47	13.58	14.93	15.19	15.47	15.55	0.02
Na_2O	1.58	1.63	1.91	1.39	1.59	2.55	2.05	1.86	2.00	2.09	2.12	2.07	0.10
K_2O	0.16	0.14	0.17	0.12	0.17	0.15	0.25	0.11	0.15	0.12	0.17	0.13	0.03
P_2O_5	0.02	0.03	0.02	0.02	0.02	0.02	0.03	0.02	0.03	0.02	0.02	0.02	0.02
LOI	0.04	−0.03	0.24	0.56	0.14	0.28	1.20	0.12	0.06	0.15	0.40	0.21	
Total	100.46	101.58	100.89	100.30	101.32	101.05	99.87	100.56	100.00	101.11	101.51	101.60	
Cu	9	13	14	55	8	5	6	8	6	2	2	3	2
Ni	267	261	139	465	225	24	31	69	0	0	0	0	3
Rb	3	3	4	3	6	2	5	4	6	5	7	7	2
Sr	296	302	352	241	278	424	429	408	364	373	401	403	2
Zr	24	21	17	20	23	16	16	16	13	14	14	15	4
Y	4	3	4	2	3	3	3	2	7	4	7	6	1
V	61	56	45	70	62	26	19	28	28	19	16	11	14
Cr	1208	1055	750	1552	1295	445	107	439	641	238	134	10	7
mg#	79.4	82.9	76.7	78.1	78.1	69.7	74.7	74.7	75.1	75.1	76.9	82.1	
IL(Zr)**	16	14	11	13	15	11	11	11	9	9	9	10	
IL(K)**	11	9	11	8	11	10	17	17	7	10	8	11	

* Depth refers to depth in metres relative to the base of the Merensky Reef. Units M and F refer to Merensky and Footwall cyclic units.
** IL refers to percentage of interstitial liquid calculated using Zr and K_2O contents, as discussed in the text.

this, and all binary plots demonstrate a well-constrained linear trend between the compositions of plagioclase and orthopyroxene (Fig. 3).

The near-adcumulate nature of these rocks is demonstrated by the low concentrations of incompatible elements, such as K_2O, P_2O_5, Rb, Zr and Y (Table 1). The range of concentrations of these elements is quite restricted. For example, the average of 167 analyses for Zr is 19 ppm, with only 17 samples falling below and 11 samples above the range of 15 to 25 ppm Zr. This suggests a remarkably uniform intercumulus component. Furthermore, there does not appear to be any significant difference between samples above and below the Merensky Reef in terms of trace elements abundances.

The variation in composition with height is illustrated in Fig. 4*a*, showing the MgO content through one vertical section. The abruptness of the modal layering can be seen by the sudden changes in MgO across boundaries, such as between footwall 6 and 5. In footwall 3 the upwards increase in MgO, which reflects increasing pyroxene content, can be seen. Individual mineral analyses have not been undertaken on all these samples. However, as orthopyroxene is the only mafic phase present the mg# (defined as 100*Mg/(Mg+total Fe)) of the whole rock and the orthopyroxene will be similar. Hence, the plot of mg# *vs.* height, shown in Fig. 4*b*, essentially illustrates the changes in orthopyroxene composition through this interval. In the anorthositic

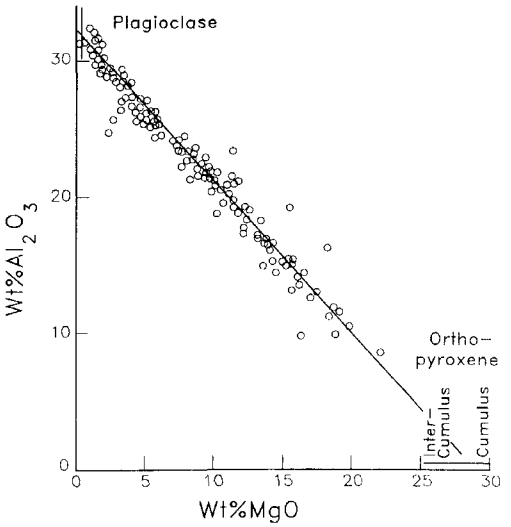

FIG. 3. Plot of whole-rock Al_2O_3 *vs.* MgO for 180 samples. Many samples with <10 wt.% MgO are not plotted because of the density of points. This plot demonstrates that the samples represent mixing between plagioclase and orthopyroxene. The compositions of typical plagioclase and orthopyroxene in this interval are shown.

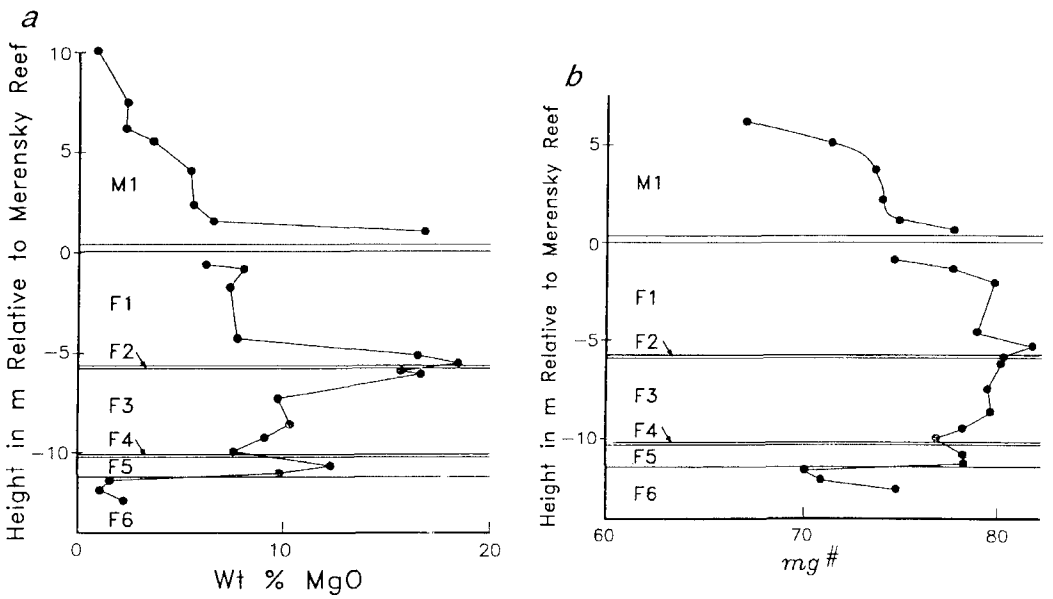

FIG. 4. Plot of height relative to the base of the Merensky Reef against whole-rock MgO (Fig. 4*a*) and mg# defined as 100*Mg/(Mg+total Fe) (Fig. 4*b*), for a single core (BS1122). Analyses are given in Table 1.

footwall 6 the mg# is much lower than in the associated more mafic rocks.

Interpretation

Several processes of petrological interest and debate can be investigated with the present information. The extent of fractionation of a liquid in a layered intrusion is usually monitored by determining mineral compositions. However, it is crucial to be able to distinguish the true cumulus composition from any intercumulus component arising from crystallization of, or reaction between, cumulus grains and interstitial liquid. Addition of magma may be recognized by sudden and sustained breaks in cumulus mineral composition or by changes in element ratios which are not sensitive to changing modal proportions of cumulus minerals. An estimation of the proportion of interstitial liquid is commonly determined from the concentration of elements incompatible in the cumulus minerals. In this regard it is also relevant to ascertain whether this liquid has been trapped in contact with the grains which formed from it, or whether it has migrated through the crystal mush. Ultimately, a hydrothermal fluid may be released from interstitial liquid which may also have a significant effect upon the final rock composition. Once all of these aspects have been evaluated it may be possible to place some constraints on liquid composition from a knowledge of cumulus mineral and whole-rock compositions.

Aspects relating to the evolution of this sequence of rocks which can be evaluated from the present data base include: the role of fluid, channelled through pothole structures; addition of magma and its contribution to cyclic layering; the composition of this liquid; migration of residual liquid within the cumulate pile, and the proportion of interstitial component.

Fluids and pothole structures. It has been suggested that potholes are the site of fumarolic activity or migration of residual fluids (Boudreau, 1992). As these postulated fluids would have been generated at lower temperature than that when the cumulate phases formed, reaction between fluid and cumulates in potholed areas could have produced geochemical differences compared with the cumulates in unpotholed areas. Based on a study of three pairs of borehole intersections through the immediate footwall to potholes and unpotholed Merensky Reef, Cawthorn and Poulton (1988) suggested that there was enrichment in mobile, incompatible elements under potholes, consistent with this hypothesis. They showed that K_2O, Rb and Cu were enriched in footwall 3 below potholes relative to adjacent unpotholed footwall 3 in two of the three profiles studied. No enrichment in immobile, incompatible

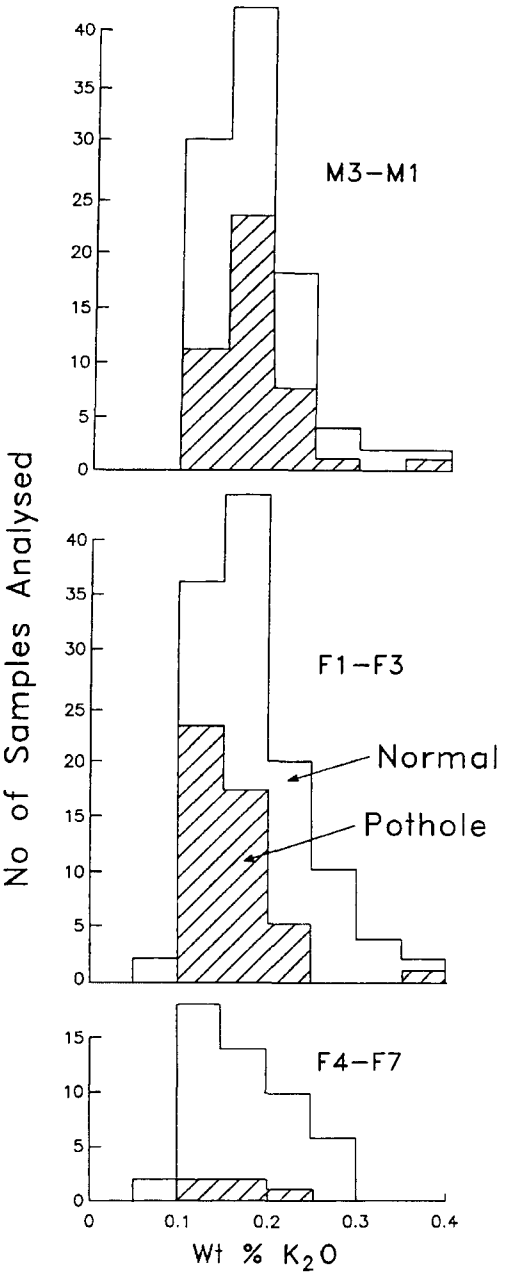

FIG. 5. Histogram of K_2O contents in the Merensky Reef cyclic unit (M1-3), immediate footwall (F1-3) and deep footwall (F4-7). Shaded samples are from bore cores intersecting potholed Merensky Reef; unshaded from normal Reef sections.

elements, such as TiO_2 and P_2O_5, was noted, and so the increase in the mobile incompatible elements was not attributable to the presence of a greater proportion of residual liquid.

In the present study a further three pairs of boreholes have been analysed. The results are presented in a histogram of K_2O contents in Fig. 5. No systematic differences in concentration are seen to exist between samples in potholed and unholed environments. Of the total database from this and the study of Cawthorn and Poulton (1988), only two of the six borehole intersections through potholed reef show enriched incompatible element abundances, and so the conclusion of Cawthorn and Poulton (1988) is not substantiated by this study. Samples from the Merensky cyclic unit show no difference in abundance between potholed and unpotholed intersections, and also contain the same average K_2O content as the footwall.

Magma addition. A geochemical break at the level of the Merensky Reef is revealed by the trends displayed on a plot of Sr *vs.* MgO (Fig. 6). This is analogous to the MgO *vs.* Al_2O_3 in Fig. 3, and shows a linear mixing trend between plagioclase and orthopyroxene. However, this diagram shows clearly that samples from above the Merensky Reef define a trend with a lower Sr content than samples from below the Reef, consistent with the conclusion of Eales *et al.* (1986) that the sequence from above the Merensky Reef formed from a magma with a different Sr content. While few Sr isotopic data are available on samples from this specific mine (Reid *et al.*, 1993), they are consistent with all other studies (e.g. Kruger and Marsh, 1982; Eales *et al.*, 1986) which show a major isotopic break at the level of the Merensky Reef, indicating addition of chemically distinct magma.

Composition of the magma. The compositions of the resident and any added magmas forming the upper Critical Zone have been extensively debated, as it has bearing on mechanisms for the formation of Merensky Reef-type mineralization. Irvine *et al.* (1983) suggested that two fundamentally different, and unrelated, magmas were interstratified within the chamber, one being highly magnesian, the other being anorthositic. Each formed its own characteristic cumulates (pyroxenite and anorthosite respectively), while mixing between them resulted in chromitite and sulphide formation. Naldrett *et al.* (1986) suggested that the magma that was intruded at the level of the Merensky Reef was magnesian and that the immediate footwall had formed from an extensively differentiated magma that had evolved from the same original composition. In these studies the UG2 cyclic unit comprising the footwall to the Merensky Reef was regarded as having been derived from a single magma. In contrast, Schurmann (1993) envisaged the involvement of six injections of a suite of magmas related to those proposed by Harmer and Sharpe (1985) to produce the sequence from footwall 13 to footwall 1 in Fig. 2.

As these rocks are cumulates formed after possible mixing of various proportions of different magmas it is difficult to determine uniquely the bulk compositions of either resident or injected magmas. However, it is possible to constrain the MgO content of the magmas by using the composition of orthopyroxene. In the entire interval from the UG2 chromitite to the Merensky Reef the most magnesian orthopyroxene is En_{83} (Naldrett *et al.*, 1986; Eales *et al.*, 1993*b*; Schurmann, 1993). It is generally accepted that these pyroxenes have formed at some stage of differentiation from a parental magma containing about 13% MgO (Cawthorn and Davies, 1983). Subsequent studies on this composition by Barnes (1986*b*) and

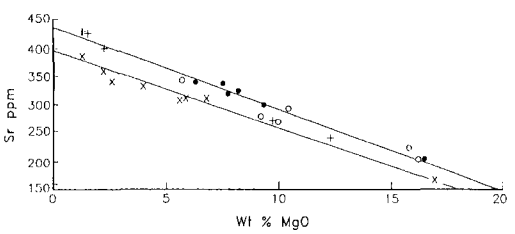

FIG. 6. Plot of whole-rock Sr *vs.* MgO for samples from one bore core (BS1122). Samples from the Merensky cyclic unit are designated with a cross. Solid dots, open dots and plus symbols refer to samples from F1–2; F3; F4–6 respectively. The upper and lower lines define trends for samples below and above the Merensky Reef respectively.

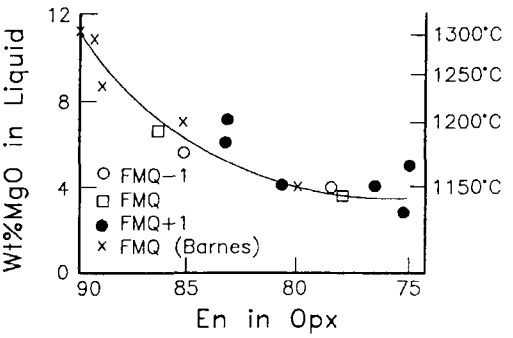

FIG. 7. Compositions of orthopyroxene and coexisting silicate liquid obtained from experimental studies at various oxygen fugacities on probable parental magma to the Bushveld Complex, based on analyses from Barnes (1986*b*, denoted by cross) and Cawthorn and Biggar (1993). An approximate temperature scale is also indicated.

Cawthorn and Biggar (1993) yielded compositions of coexisting orthopyroxene and silicate liquid. The relevant results are summarized in Table 2 and Fig. 7. These show that the magma in equilibrium with En_{83} contains only 5 to 6% MgO. Thus the magma from which the pyroxenite of the upper Critical Zone formed is far from being highly magnesian. The same experimental data also show that such a magma will also be saturated with plagioclase, a conclusion presented by Eales *et al.* (1988) using trace element contents of orthopyroxene.

Migration of residual magma. Reaction between primary orthopyroxene and trapped residual liquid causes the En content to decrease. If there had been

TABLE 2. Co-existing pyroxene and liquid compositions

Previously unpublished analyses from experimental study of Cawthorn and Biggar (1993)

Temp °C	1283	1281	1205	1184	1184	1139	1139
Buffer*	fmq−1	fmq+1	fmq	fmq−1	fmq+1	fmq−1	fmq+1
Liquid compositions							
SiO_2	56.65	57.26	57.43	58.46	57.01	61.53	59.32
TiO_2	0.39	0.38	0.44	0.45	0.45	0.90	0.91
Al_2O_3	12.52	12.46	14.20	14.59	14.75	14.65	13.16
FeO	7.52	8.20	7.67	6.68	7.64	6.32	7.18
MnO	0.17	0.17	0.15	0.14	0.14	0.09	0.11
MgO	8.40	9.42	6.44	5.24	5.74	2.92	3.99
CaO	6.91	6.72	7.84	7.92	7.92	6.06	7.01
Na_2O	2.90	2.49	2.54	2.72	2.68	2.42	1.75
K_2O	2.79	2.17	1.81	2.36	1.98	3.23	2.16
P_2O_5	0.25	0.29	0.24	0.31	0.35	0.41	0.30
Cr_2O_3	0.11	0.07	0.04	0.05	0.08	0.03	0.02
Total	98.61	99.63	98.80	98.92	98.74	98.56	95.90
mg#(L)	66.6	67.2	60.0	58.3	57.2	45.2	49.8
Phase**	Ol	Ol	Opx	Opx	Opx	Opx	Opx
SiO_2	39.75	40.50	55.91	53.25	56.03	54.81	54.28
TiO_2	–	–	0.07	0.09	0.10	0.10	0.10
Al_2O_3	0.05	0.10	1.30	1.45	0.88	0.80	0.95
Cr_2O_3	0.11	0.10	0.34	0.69	0.22	0.09	0.17
FeO	12.07	9.60	8.95	15.79	9.72	15.23	14.31
MnO	0.23	0.19	0.20	0.24	0.24	0.30	0.30
MgO	47.05	49.65	31.85	26.64	31.52	27.80	29.35
CaO	0.30	0.21	1.37	0.90	1.18	0.80	0.90
Total	99.56	100.35	99.99	99.05	99.89	99.93	100.36
mg#	87.42	90.21	86.38	75.04	85.25	76.49	78.52

Summary of MgO and FeO contents of liquids and mg# in orthopyroxene from study of Barnes (1986*b*)

Temp °C	1334	1299	1264	1254	1209	1158
Buffer	fmq	fmq	fmq	fmq	fmq	fmq
MgO(L)	13.51	11.17	10.99	8.76	7.29	4.01
FeO(L)	9.15	7.93	8.54	7.33	8.23	7.86
mg#(L)	72.4	71.5	69.6	68.0	61.2	47.6
mg#(Opx)	90.40	90.85	89.70	89.04	86.65	80.20

Buffer * — f_{O_2} relative to fayalite–magnetite–quartz buffer
Phase ** Ol — olivine, Opx — orthopyroxene

migration of such liquid across a boundary where a reversal in composition has taken place then pyroxene occurring above such a reversal would have had its En content decreased by reaction with highly differentiated liquid (Irvine, 1980). Alternatively, if migration of liquid had taken place across a boundary where there was a sudden decrease in the primary En content of the pyroxene, reaction would have increased the En value in the pyroxene immediately above such a break. Thus total variations in primary En content within a short vertical interval would have been reduced by infiltration processes.

The pyroxene compositions from the UG2 chromitite to the top of the Merensky cyclic unit are shown in Fig. 8. Two apparent differentiation sequences with an intervening regression might be inferred from these values. Between the top of the footwall and the base of the Merensky Reef there is a change in En content from 68 to 81 over a vertical interval of 2 metres in the Union Mine profile, from 77 to 83 in the Rustenburg Mine profile, and from 76 to 79 (for whole-rock mg#) in the Impala Platinum Mines profile (Fig. 4*b*). Had there significant upward migration of residual liquid from footwall cumulates into the Merensky Reef such sharp breaks would not have been preserved. Furthermore, the lowermost cumulates of the Merensky Reef would show an upward increase in En content concomitant with the diminishing influence of upward-migrating liquid (Irvine, 1980). Downward migration of dense residual magma from the Merensky Reef into the footwall would have caused an increase in En values in pyroxene in the immediate footwall. Neither trend is observed. Thus, these data argue against migration of residual magma.

The data of Naldrett *et al.* (1986) and those presented here can be treated quantitatively to examine the influence of residual magma. Naldrett *et al.* (1986) attributed the trends shown in Fig. 8 to fractional crystallization, with the cyclic unit from the top of the UG2 to the base of the Merensky Reef forming from a single magma. This conclusion ignored the fact that the An content of the plagioclase actually increased upwards through this same section.

A detailed study of one layer within the UG2 cyclic unit, the noritic footwall 7, shows that the En content of the pyroxene remains constant for over

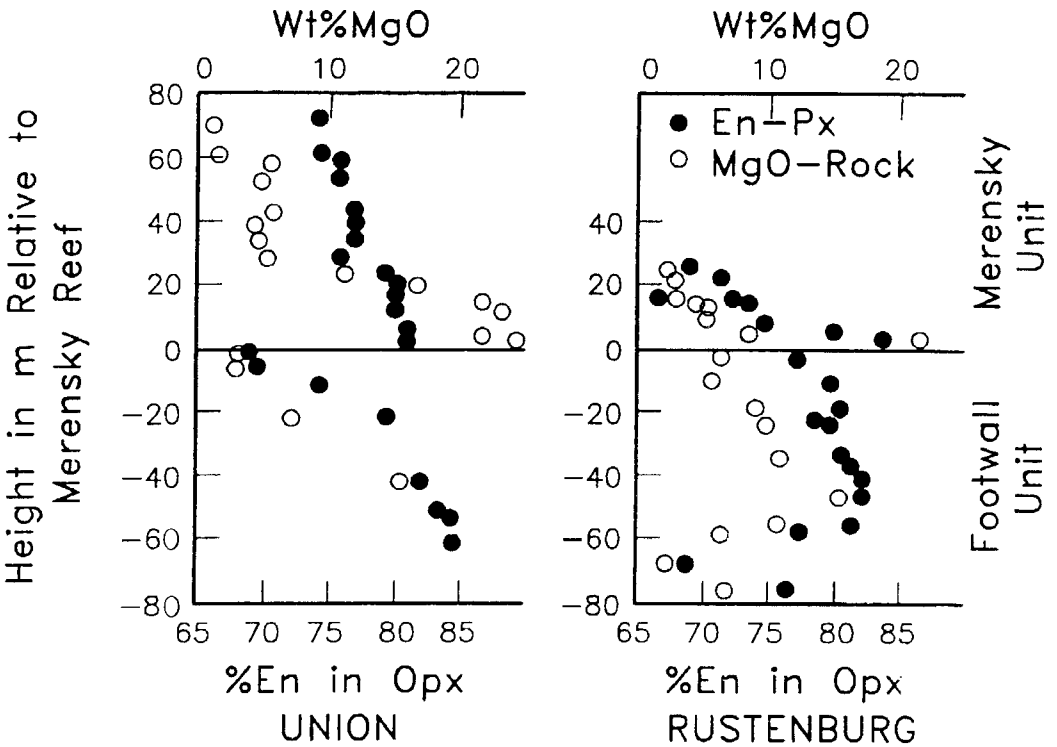

FIG. 8. Plot of En content of orthopyroxene (solid dots) and MgO content of whole-rock samples (open dots) as a function of height relative to the Merensky Reef in the upper Critical Zone for two profiles some 70 km apart (taken from the study of Naldrett *et al.*, 1986).

40 m (Fig. 9). In contrast, the more detailed study of footwall 1 to 6 (Fig. 4), indicates that there are reversals in the mg# within each cycle. Also, footwall 3 shows an upwards increase in mg# as the unit becomes more mafic. In another section (Fig. 10), it can be seen that there are sudden dramatic decreases in the mg#. For example, at the contact between the noritic footwall 7 and the anorthositic footwall 6 the mg# decreases from a uniform value of 81 to less than 60, within 30 cm. A similar decrease is seen at the base of footwall 4. Thus an examination of the details within this cyclic unit reveals that whereas there appears to be an overall upward differentiation in terms of En content of the pyroxene, there are considerable thicknesses which show no differentiation; others which show abrupt reversals; and yet others with extremely sharp forward displacements in the differentiation index. Such observations would seem to require extremely complicated processes occurring within the magma.

Reference to Figs 4, 8 and 9 shows that there is a good correlation between En in orthopyroxene or mg# of the whole rock and the MgO content of the whole rock. Given the major vertical variations in modal proportion of plagioclase to pyroxene shown in Fig. 2, this is difficult to explain in terms of fractionation from a single magma. The models of Naldrett *et al.* (1986) and Schurmann (1993) assume that the composition of the pyroxene is that of the primary mineral. If there is reaction between primary phase and residual liquid this need not necessarily be correct. In the extreme case where the primary minerals trap the residual liquid from which they formed, Barnes (1986*a*) showed that the extent of change of the mineral composition varied with the relative proportions of the primary phase and trapped liquid, and in the case of pyroxene the MgO and FeO content of the trapped liquid. This model predicts that the biggest shift in the En content of the pyroxene to lower En values should occur in the anorthositic (low MgO) rocks, exactly as is observed.

The above argument assumes that there has been no vertical migration of magma. This can be confirmed from this data set. In Fig. 10 the whole-rock mg# decreases from 81 to less than 60 over a vertical interval of 30 cm, in moving from a norite to an anorthosite. If residual liquid had migrated upwards, the lowest sample immediately above this sharp break would have been infiltrated by liquid with a high mg# value and would therefore have been reset to higher values. As this rock is an anorthosite with very little pyroxene such resetting would have been easily accomplished. The preservation of such a sharp break at the boundary clearly demonstrates that no residual magma migrated upwards, even on a scale of 30 cm.

Evaluating the possibility of downward migration of residual magma can be attempted using the data of Kruger and Marsh (1982) and Eales *et al.* (1986). Kruger and Marsh (1982) used the initial Sr isotopic ratio to demonstrate that the Merensky Reef had formed from a magma isotopically distinct from its footwall. The sudden increase in this ratio occurred at and immediately above the base of the Reef. There is no evidence in their data, even for samples <1 m below the Reef, that the ratio began to increase below the Reef as would be expected if downward infiltration of a liquid with a higher ratio had occurred. The same argument can be used for the Sr/Al_2O_3 ratio plot of Eales *et al.* (1986) where sharp breaks occur at the bases of all five cyclic units studied.

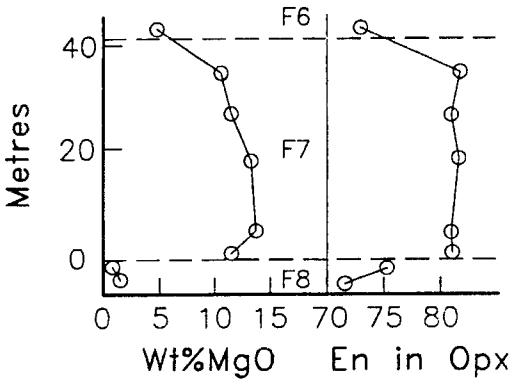

FIG. 9. Plot of vertical height in footwall unit 7 and its adjacent units *vs.* whole-rock MgO content and En content of orthopyroxene (from Schurmann, 1993). The pyroxene is of uniform composition throughout the entire 40 m of the noritic footwall 7, but is distinctly depleted in En in the over- and underlying anorthositic layers.

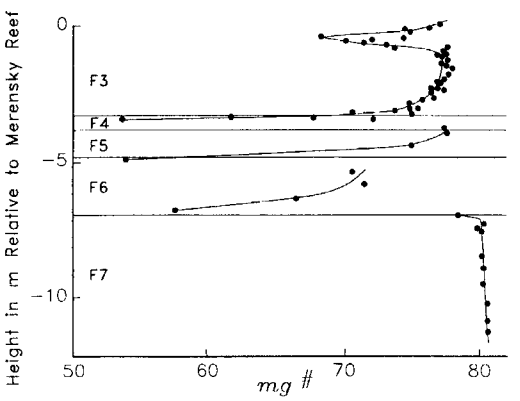

FIG. 10. Plot of whole-rock height *vs.* mg# in footwall units 3–7, sampled at 20cm intervals. There are extremely sudden breaks in mg# between adjacent units.

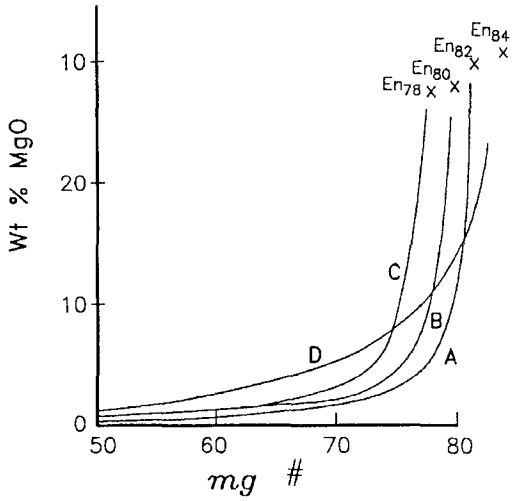

FIG. 11. Calculated curves showing the whole-rock MgO and mg# compositions based on the trapped liquid shift model of Barnes (1986*a*). The curves A, B and C describe the change in bulk composition for primary pyroxenes with compositions En_{82}, En_{80} and En_{78} respectively, with a constant proportion of 10% trapped liquid. As the ratio of primary pyroxene to plagioclase decreases, both MgO and mg# decrease with a hyperbolic relationship. For curve D, 30% trapped liquid and a primary pyroxene composition of En_{84} are assumed.

Composition of parental magma and cumulus pyroxene. Exact calculations of the trapped liquid shift effect on pyroxene compositions for the present suite of rocks are simple as the system involves plagioclase with zero MgO and FeO, pyroxene and liquid. Furthermore, the MgO and FeO contents of the liquid have been constrained from experimental studies mentioned above (Table 2). It is possible, therefore, to calculate any bulk-rock MgO and FeO content, and hence mg#, assuming varying proportions of plagioclase, pyroxene and liquid. Examples of modelled calculations are shown in Fig. 11. Trapped liquid proportions of 10 and 30% are used in these calculations. If there is only 10% trapped liquid (curves A to C; Fig. 11), then the mg# for the bulk rock changes very little as the proportion of primary pyroxene changes from 90 to 30% (equivalent to 30–10% whole-rock MgO). However, at lower proportions of primary pyroxene major shifts in mg# are predicted. The curve for 30% trapped liquid displays a more gradual change in the whole-rock mg#.

The results obtained by Naldrett *et al.* (1986) and in this study are shown in Figs 12 to 14. In all of these diagrams it can be seen that the data plot along the general trends predicted by the curves calculated in Fig. 11. In Fig. 12 the data of Naldrett *et al.* (1986) show that the actual pyroxene compositions straddle curve C in Fig. 11. Thus the variation in En content in pyroxene and the correlation between En content and whole-rock MgO for the entire UG2 cyclic unit can be attributed entirely to reaction between a constant proportion of trapped liquid with variable

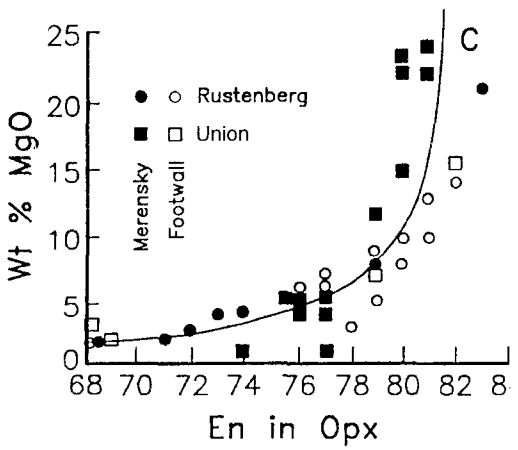

FIG. 12. Plot of whole-rock MgO content *vs.* En value of pyroxene (from Naldrett *et al.*, 1986). The curve C is taken from Fig. 11. There is good agreement between the data and the model curve. Samples from the Merensky unit (filled symbols) generally have lower En contents than footwall samples (open symbols).

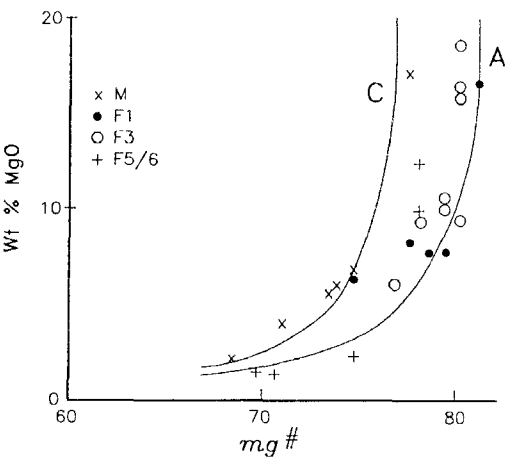

FIG. 13. Plot of whole-rock MgO content *vs.* mg# for bore core BS1122. Curves A and C are the same curves as calculated in Fig. 11. Samples from the Merensky unit (M), shown by crosses, plot at lower mg# values than footwall samples (F).

proportions of orthopyroxene having constant primary compositions. The pyroxene-rich samples (i.e. high MgO) from the Merensky Reef unit generally plot at lower En contents than the samples in the footwall. Exactly the same interpretation emerges for the data presented in Fig. 13, taken from a single vertical section from this study.

Figure 14 is a composite of all sections studied here, and includes 202 analyses. Curve B from Fig. 11 is used as a discriminant. Of 95 analyses from the Merensky Reef unit, all but eight plot on the low mg# side of this curve, whereas of the 107 footwall analyses, all but 10 plot to the high mg# side. Hence, it can be concluded that there is a distinct difference in primary pyroxene composition between footwall and Merensky units, and that the Merensky unit has the lower mg# value. Kruger (1992) reached a rather similar conclusion.

The shape and position of the various curves defined by the data can be compared with modelled curves in Fig. 11 to indicate both the composition of the primary pyroxene and the proportion of trapped liquid. Footwall samples in Fig. 13 define a curve similar to curve A in Fig. 11, and hence indicate that the primary pyroxene at that level had a composition En_{82}. From this it is concluded that the liquid from which the pyroxene crystallized contained 5–6% MgO (Fig. 7). The data from the Merensky unit define a curve similar to curve C in Fig. 11, and so project back to a primary pyroxene composition of En_{80}, indicating a liquid with only 4–5% MgO.

Vertical sections where the modal proportion of pyroxene is constant have uniform pyroxene composition or constant whole-rock mg#, even in thick sequences (Fig. 9) . Where modal pyroxene decreases upwards, so does the apparent En (or whole-rock mg#) content, even over very short vertical sections (Ml in Fig. 4). An upwards increase in modal pyroxene content correlates with an increase in En or mg# (F3 in Fig. 10). Extremely sharp breaks in En or mg# value simply reflect equally sudden changes in mode (between F7 and F6 in Fig. 10). All these features are predicted by the trapped liquid shift effect. There is no need to appeal to complicated and frequent sequences of magma input and mixing, and variable amounts of fractionation over very short vertical intervals to explain the variations in mineral chemistry. It is concluded, therefore, that there was no significant systematic cryptic variation in the original pyroxene compositions within the UG2 cyclic unit.

Migration of sulphide liquid. The ideal tracer for identifying migration of residual liquid would be one which was chemically very distinct, had a high density contrast with the surrounding cumulates, had low viscosity, and only crystallized at temperatures below the solidus of the silicate cumulates. Such a tracer exists, namely the sulphide liquid which formed at the base of the Merensky Reef. Its high Cu content makes it chemically distinct. It has a very high density and low viscosity in relation to its surroundings. It separated as an immiscible liquid at magmatic temperatures, but even at temperatures down to 1000°C the data of Fleet *et al.* (1993) show that it would be only about 50% crystallized. The sulphide occurs primarily in the pyroxenite of the Merensky Reef, but in Impala Platinum Mines it is also present in the footwall. The extent of this can be seen by a plot of Cu content *vs.* depth below the Merensky in Fig. 15. Similar trends are noted for the sulphur content in this suite of rocks, demonstrating that the Cu is associated with sulphide. However, as the precision on analysis for sulphur is lower than for Cu, the data for Cu are used preferentially to illustrate the behaviour of the sulphide. Immediately beneath normal Reef, Cu contents reach over 1000 ppm, decreasing to values of less than 50 ppm within less than 5 m. At greater depth, values remain at less than 50 ppm, which is typical of the entire footwall unit down to the UG2 chromitite (Schurmann, 1993). Assuming that it separated at the same time as the Merensky Reef, these results indicate that the sulphide sank less than 5 m into the crystal pile. As listed above, the physical properties of this sulphide liquid are such that it should be capable of migrating through interstitial space far more effectively than a silicate liquid. The implication is that the latter would have migrated only extremely short distances.

Of significance in Fig. 15 is the fact that the footwall of potholed Reef shows enrichment in Cu of only a factor of two, and only over ~2 m, relative to its deeper footwall. In the present study only profiles intersecting potholes which bottom against footwall 3 have been analysed. Two models have been proposed for pothole formation, and may be examined in the light of the present data. In one they are thought to have originated at the site of upwelling fluid or residual liquid (Boudreau, 1992). Copper and the platinum-group elements are inferred to have been introduced by this fluid. However, it is noted that Cu is depleted (Fig. 15) in the footwall to potholed Reef compared with that beneath normal Reef. If they were the channelways for such processes they might be expected to contain higher proportions of interstitial magma and fluid and so be preferentially permeable compared with normal profiles. Such a situation would lead to greater, not lower, Cu contents in the footwall to potholes.

The second general model for the formation of potholes attributes them to the physical removal of the immediate footwall layers either by mechanical or thermal mechanisms (Campbell, 1986). If this has occurred it is reasonable to assume that footwall 3 would have been more consolidated than footwall 1

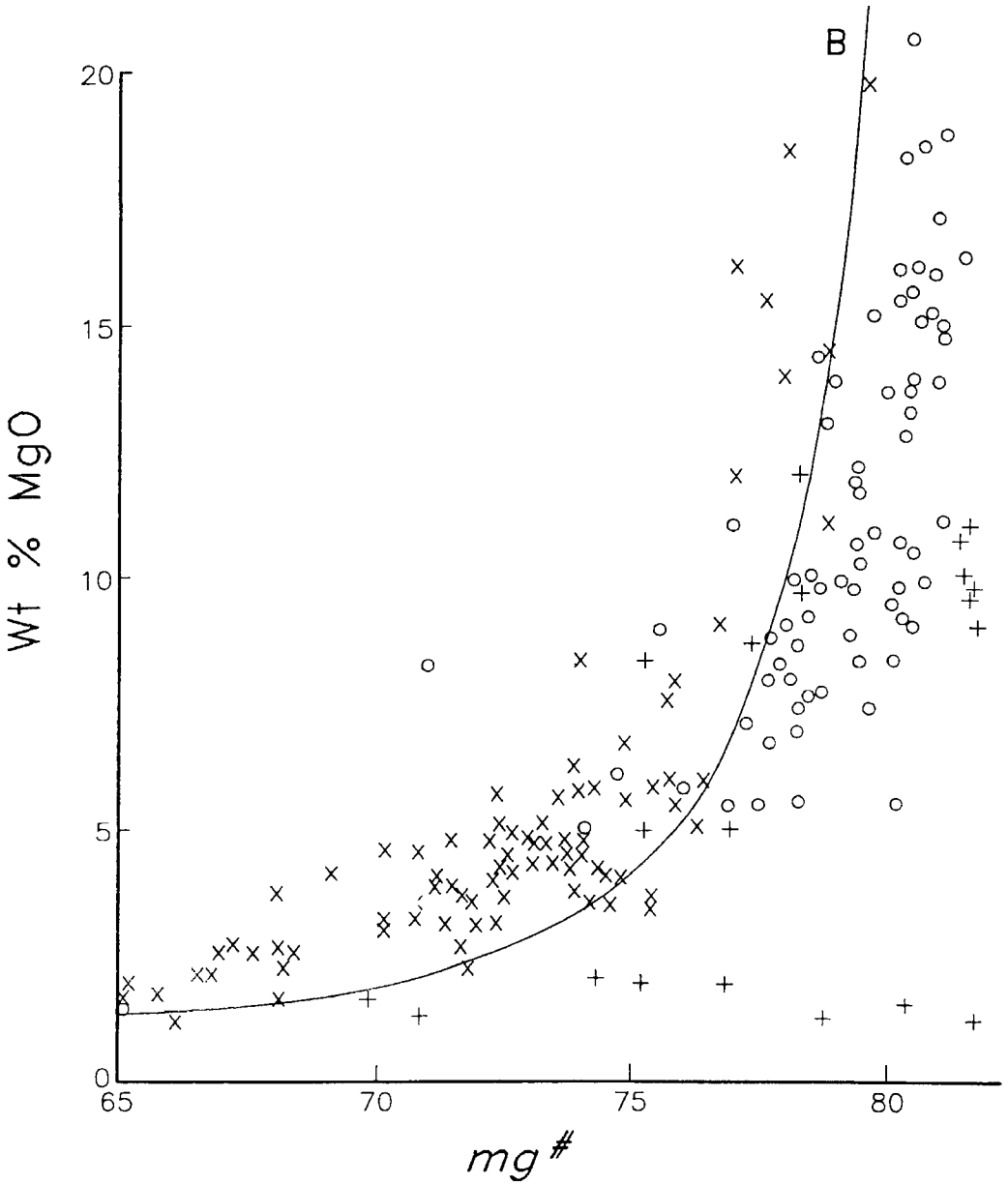

FIG. 14. Plot of whole-rock MgO content *vs.* mg# for all ten bore core intersections, totalling 202 samples. Sample designation as in Fig. 13. Curve B is taken from Fig. 11.

at the time the pothole developed. At the time that the Merensky Reef and its sulphide began to accumulate, footwall 1 would have had higher permeability than the re-exhumed footwall 3 at the base of the pothole. The lack of enrichment of Cu below potholes in Fig. 15 suggests that sulphide was unable to penetrate far into footwall 3. It must therefore have been impermeable even to a sulphide liquid, even though it was <10 m below the original liquid–cumulate interface. Adcumulates, therefore, may form very close to this boundary by textural annealing, as demonstrated by Walker *et al.* (1988), rather than by

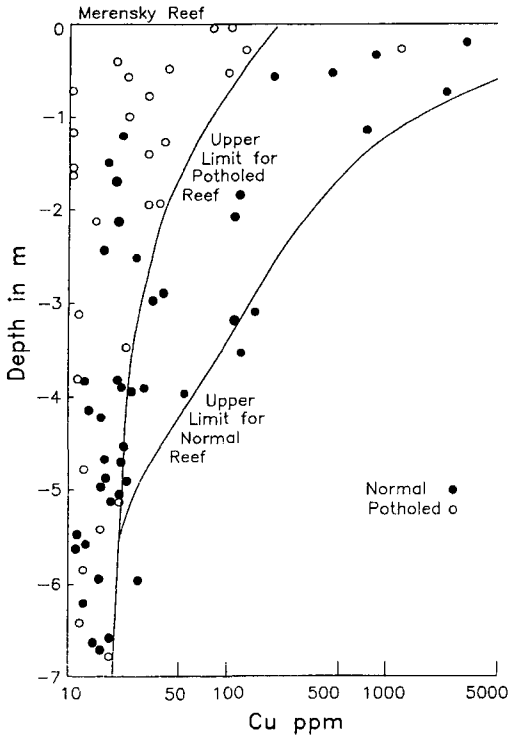

FIG. 15. Plot of Cu content *vs.* depth below the Merensky Reef for samples taken from ten bore cores. A log scale is used for the Cu content. Samples from potholed and normal Reef are distinguished. The curves indicate the upper limits of Cu for the two settings.

infiltration of liquid through substantial thicknesses of crystal mush.

Proportion of interstitial liquid. The shapes of the curves in Figs 12 and 13 are closer to the calculated curves for 10% rather than 30% trapped liquid (c.f. Fig. 11), and so indicate relatively low interstitial liquid content. These diagrams are interpreted to imply that all the rocks from the footwall sequence contained the same primary pyroxene composition, and the same proportion of trapped liquid and varied only in their plagioclase to pyroxene ratio. If this is correct it should be possible to take every whole-rock analysis, subtract the fixed proportion of liquid (10%), and determine the primary mg# or En content of the pyroxene. The MgO and FeO contents of the magma used in this calculation are taken from Table 2. This has been done in Fig. 16, for the data presented in Fig. 4. A remarkably uniform mg# value is obtained for the entire footwall sequence, supporting the validity of this argument. In Fig. 4*b* the mg# value in footwall 1 to 6 varies from 70 to 83, whereas in Fig. 16 this range is reduced to 79–84. Had the proportion of trapped liquid been highly variable, greater variability of mg# values would have resulted in the calculations shown in Fig. 16. Had the proportion of trapped liquid been higher, this calculation would have resulted in unrealistically high mg# values for leucocratic rocks. Had there been a lower proportion this would have resulted in leucocratic rocks still having anomalously low mg# values as seen in the raw data (Fig. 4*b*).

Determination of the trapped liquid content based on the degree of curvature in diagrams such as Figs 12 and 13 is not reliable without other evidence. Trapped liquid content can also be estimated using the abundances of incompatible elements. The whole-rock content of Zr and K_2O can also be used to estimate the trapped liquid content. In order to do this it is necessary to infer a concentration for these elements in the liquid. Values of 150 ppm Zr and 1.5% K_2O have been used. These are double the values determined for the parental magma to the Bushveld Complex, as 50% fractionation has been inferred from the experimental studies reported in Fig. 7. The proportion of interstitial liquid calculated in this way is given in Table 1, and averages about 10%. Using these proportions of trapped liquid, primary mg# values have been calculated in Fig. 16. The constancy of the calculated proportions of trapped liquid from incompatible elements and those inferred from the curvature in Figs 12 and 13 suggests that this is a reasonable estimate for this suite of rocks.

For these calculations, shown in Table 1 and Fig. 16, a constant composition of the trapped liquid has been assumed. This is considered a reasonable approximation for two reasons. A vertical interval of less than 25 m is being considered, which is trivial compared with the total thickness of the entire intrusion. Furthermore, it has been demonstrated in the above discussion that the composition of the cumulus pyroxene remained virtually constant throughout this interval. Both these observations indicate that very little fractionation had taken place through the interval considered and so little increase in incompatible element abundances of the residual liquid would be expected.

The data in Fig. 16 show that most footwall samples have a fairly constant mg# value greater than 79, whereas samples from the Merensky cyclic unit show lower and rapidly decreasing mg# values. This suggests that rapid differentiation or mixing with more evolved magma is taking place during the formation of this interval.

Conclusions

The rock sequence from the Upper Group 2 chromitite to the Merensky Reef is not a simple cyclic unit. It contains 13 distinct layers with variable

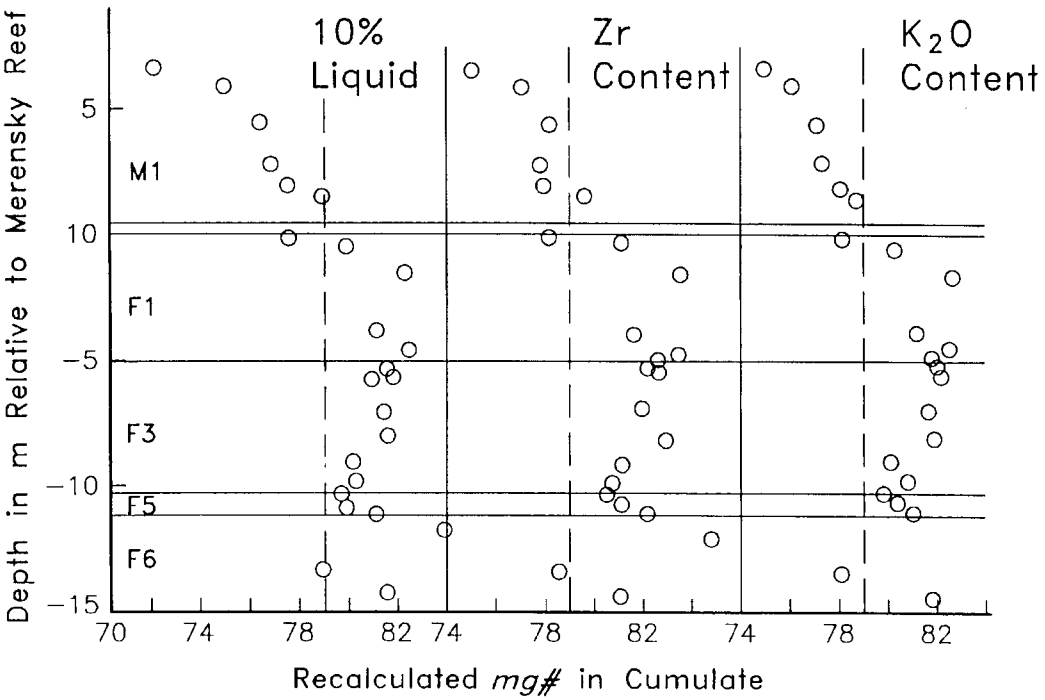

FIG. 16. Plot of height relative to the base of the Merensky Reef *vs.* recalculated whole-rock mg# value. In the first column a uniform 10% trapped liquid in all samples has been assumed, removed from the whole-rock analysis and the primary mg# value determined. In the next two columns the proportion of trapped liquid has been calculated from the abundance of Zr and K_2O respectively (Table 1), and again subtracted from whole-rock composition to give primary mg# values. A reference line at a mg# value of 79 has been included in all diagrams. Nearly all footwall samples have higher mg# values than this, whereas samples from the Merensky cyclic unit have lower values.

proportions of plagioclase to pyroxene. Similarly, the trend of mg# content in pyroxene and whole rock is not smooth. Forward and reverse breaks may occur over very short vertical intervals, but variations always correlate with modal abundance of pyroxene. Reversals occur where modal pyroxene increases, and forward breaks where pyroxene decreases. Such observations are difficult to explain if these compositions are taken to reflect primary mineral compositions. However, they are totally predictable if a constant primary pyroxene composition of En_{82} is assumed and observed variations are related to the trapped liquid shift effect.

The entire UG2 cyclic unit, which is over 100 m thick, contains pyroxene which had a near-constant composition. This implies that it crystallized from an extremely large reservoir of magma. In contrast, in 20 m of the overlying Merensky Reef unit there is evidence of considerable differentiation or magma mixing.

Experimental evidence from the orthopyroxene compositions indicates that the Merensky Reef and its footwall did not form from a primitive or highly magnesian liquid, but from liquids with 4–6% MgO. Furthermore, the Merensky Reef liquid was more evolved than the footwall magma.

The only evidence for migration of liquid that can be identified is of downward migration of an immiscible sulphide liquid. This has migrated less than 5 m into the footwall of the Merensky Reef despite its very high density contrast with silicate liquid, low viscosity and low crystallization temperature, all of which should facilitate infiltration.

Two independent techniques for estimating the proportion of trapped liquid yield values of about 10%.

These observations and conclusions are probably a consequence of the extremely slow crystallization and accumulation rates of this enormous intrusion, permitting the post-cumulus processes of compaction and annealing to take place close to the crystal-liquid interface. They may not apply in shallow-level and small bodies.

Acknowledgements

Access to bore core samples, courtesy of the Genmin and Impala Platinum Mines, and their permission to publish these results, are very gratefully acknowledged. I thank my wife and Ms S. Hall for crushing and analysing samples, and Ms L. Whitfield and D. du Toit for preparing diagrams. Reviews by B. Robins, A.E. Boudreau, S.J. Edwards and C.M.B. Henderson have, hopefully, helped to clarify many of the arguments presented here. Financial assistance was provided by Foundation for Research Development (South Africa).

References

Barnes, S.J. (1986*a*) The effect of trapped liquid crystallization on cumulus mineral compositions in layered intrusions. *Contrib. Mineral. Petrol.*, **93**, 524–31.

Barnes, S.J. (1986*b*) The distribution of chromium among orthopyroxene, spinel and silicate liquid at atmospheric pressure. *Geochim. Cosmochim. Acta*, **50**, 1889–909.

Boudreau, A.E, (1992) Volatile fluid overpressure in layered intrusions and the formation of potholes. *Austral. J. Earth Sci.*, **39**, 277–87.

Campbell, I.H. (1986) A fluid dynamic model for the potholes of the Merensky Reef. *Econ. Geol.*, **81**, 1118–25.

Cawthorn, R.G. and Biggar, G.M. (1993) Crystallization of titaniferous chromite, magnesian ilmenite and armalcolite in tholeiitic suites in the Karoo Igneous Province. *Contrib. Mineral. Petrol.*, **114**, 221–35.

Cawthorn, R.G. and Davies, G. (1983) Experimental data at 3 kbars pressure on parental magma to the Bushveld Complex. *Contrib. Mineral. Petrol.*, **52**, 81–9.

Cawthorn, R.G. and Poulton, K.L. (1988) Evidence for fluid in the footwall beneath potholes in the Merensky Reef of the Bushveld Complex. In *Geoplatinum 87* (H.M. Prichard, P.J. Potts, J.F.W. Bowles and S.J. Cribb, eds.) Elsevier, London, 343–56.

Eales, H.V., Marsh, J.S., Mitchell, A.A., deKlerk, W. J., Kruger, F.J. and Field, M. (1986) Some geochemical constraints upon models for the crystallization of the upper Critical Zone — Main Zone interval, northwestern Bushveld Complex. *Mineral. Mag.*, **50**, 567–82.

Eales, H.V., Field, M., de Klerk, W.J. and Scoon, R. (1988) Regional trends of chemical variation and thermal erosion in the upper Critical Zone, western Bushveld Complex. *Mineral. Mag.*, **50**, 63–79.

Eales, H.V., Botha, W.J., Hattingh, P.J., De Klerk, W.J., Maier, W.D. and Odgers, A.T. (1993*a*) The mafic rocks of the Bushveld Complex: a review of emplacement and crystallization history, and mineralization, in the light of new data. *J. Afr. Earth Sci.*, **16**, 121–42.

Eales, H.V., Teigler, B. and Maier, W.D. (1993*b*) Cryptic variations of minor elements Al, Cr, and Mn in Lower and Critical Zone orthopyroxenes of the western Bushveld Complex. *Mineral. Mag.*, **57**, 257–64.

Fleet, M.E., Chryssoulis, S.L., Stone, WE. and Weisener, C.G. (1993) Partitioning of platinum-group elements and Au in the Fe-Ni-Cu-S system: experiments on the fractional crystallization of sulphide melt. *Contrib. Mineral. Petrol.*, **115**, 36–44.

Harmer, J. and Sharpe, M.R. (1985) Field relations and strontium isotope systematics of the marginal rocks of the Eastern Bushveld Complex. *Econ. Geol.*, **80**, 813–37.

Irvine, T.N. (1980) Magmatic infiltration metasomatism, double-diffusive fractional crystallization, and adcumulus growth in the Muskox intrusion and other layered intrusions. In *Physics of Magmatic Processes*. (R.B. Hargraves, ed.). Princeton University Press, Princeton, New Jersey, 326–83.

Irvine, T.N., Keith, D.W. and Todd, S.G. (1983) The J-M platinum-palladium reef of the Stillwater Complex, Montana. II. Origin by double-diffusive convective magma mixing and implications for the Bushveld Complex. *Econ. Geol.*, **78**, 1287–334.

Kruger, F.J. (1992) The origin of the Merensky Reef cyclic unit: Sr-isotopic and mineralogical evidence for an alternative orthomagmatic model. *Austral. J. Earth Sci.*, **39**, 255–61.

Kruger, F.J. and Marsh, J.S. (1982) Significance of $^{87}Sr/^{86}Sr$ ratios in the Merensky Cyclic Unit of the Bushveld Complex. *Nature*, **298**, 53–5.

Leeb-du Toit, A. (1986) The Impala platinum mines. In *Mineral Deposits of Southern Africa, vol. 2* (C.R. Anhaeusser and S. Maske, eds.) Geol. Soc. S. Afr., Johannesburg, 1091–106.

McKenzie, D.P. (1984) The generation and compaction of partially molten rock. *J. Petrol.*, **25**, 713–65.

Naldrett, A.J., Gasparrini, E.C., Barnes, S.J., von Gruenewaldt, G. and Sharpe, M.R. (1986) The upper Critical Zone of the Bushveld Complex and a model for the origin of Merensky-type ores. *Econ. Geol.*, **81**, 1105–18.

Reid, D.L., Cawthorn, R.G., Kruger, F.J. and Tredoux, M. (1993) Isotope and trace element patterns below the Merensky Reef, Bushveld Complex, South Africa: evidence for fluids? *Chem. Geol.*, **106**, 171–86.

Robins, B. (1982) Finger structures in the Lille Kufjord layered intrusion, Finmark, northern Norway. *Contrib. Mineral. Petrol.*, **81**, 290–5.

Schurmann, L.W. (1993) The geochemistry and petrology of the upper Critical Zone of the

Boshoek section of the western Bushveld Complex. *Geol. Surv. S. Afr. Bull.*, **113**, 88 pp.

Tait, S.R. and Jaupart, C. (1992) Compositional convection in a reactive crystalline mush and melt differentiation. *J. Geophys. Res.*, **97**, 6735–56.

Tait, S.R., Huppert, H.E. and Sparks, R.S.J. (1984) The role of compositional convection in the formation of adcumulate rocks. *Lithos*, **17**, 139–46.

Wager, L.R., Brown, G.M. and Wadsworth, W.J. (1960) Types of igneous cumulates. *J. Petrol.*, **1**, 73–85.

Walker, D., Jurewitz, S. and Watson, E.B. (1988) Adcumulus growth in a laboratory thermal gradient. *Contrib. Mineral. Petrol.*, **99**, 306–19.

[*Revised manuscript received 10 July 1995*]